Analytical Methods

Cite this: *Anal. Methods*, 2012, **4**, 619

www.rsc.org/methods

COMMUNICATION

Anatase TiO_2 nanoparticle–graphene nanocomposites: One-step preparation and their enhanced direct electrochemistry of hemoglobin†‡

Qingming Shen, Shiwei Zhou, Xiaomei Zhao, Li-Ping Jiang,* Wenhua Hou and Jun-Jie Zhu

Received 15th November 2011, Accepted 20th January 2012
DOI: 10.1039/c2ay05781f

Anatase TiO_2 nanoparticle–graphene nanocomposites with enhanced direct electrochemistry of hemoglobin and biosensing for H_2O_2 were synthesized *via* a facile, one-step approach in aqueous solution at room temperature.

As one of the ideal electrode materials with high surface area and high carrier mobility, both graphene (GR) and its composites have attracted extensive interest for wide applications in the field of electrochemical, optoelectronic, and biosensing.[1–4] Among them, TiO_2–GR nanocomposites have triggered enormous interest from the perspective of science and technology.[5–9] Recently, several approaches for the preparation of TiO_2–GR nanocomposites have been reported, including chemical, hydrothermal, photocatalytic methods, and so on.[5–9] Generally, most of these methods involve two steps: reduction of graphene oxide (GO) to GR followed by the immobilization of TiO_2 nanoparticles, or in inverse order, which leads to relatively complicated operation and low production.[5–8] Therefore, it is necessary to develop a simple and effective method to prepare TiO_2–GR nanocomposites.[9,10]

In this paper, we present a one-step approach for the preparation of anatase TiO_2–graphene (ATG) nanocomposites using titanium(III) ion as reductant and titanium source in an aqueous solution. The high surface area, excellent conductivity and sufficiently functional groups enable the ATG nanocomposites to be favourable for fabricating biosensors. The results indicated that Hemoglobin (Hb) immoblized on ATG could realize the enhanced direct electron transfer (DET) of Hb, and Hb–ATG nanohybrid exhibited good electrocatalytic activity toward the reduction of H_2O_2.

$TiCl_3$ and GO were used as the starting materials, and the brown GO solution turned black on contact with $TiCl_3$, showing the GO nanosheets were reduced by titanium(III) ion immediately. The reaction intermediate titanium(IV) ion was then *in situ* rapidly hydrolysised to TiO_2 nanoparticles on the GR sheets. The possible reaction equation can be considered as follows:

$$Ti^{3+} + GO \rightarrow TiO^{2+} + GR \quad (1)$$

$$TiO^{2+} + H_2O \rightarrow TiO_2 + 2H^+ \quad (2)$$

Fig. 1a displays the typical transmission electron microscope (TEM) image of ATG. The tiny nanoparticles are uniformly distributed on 2D GR sheets, showing the good immobilization of

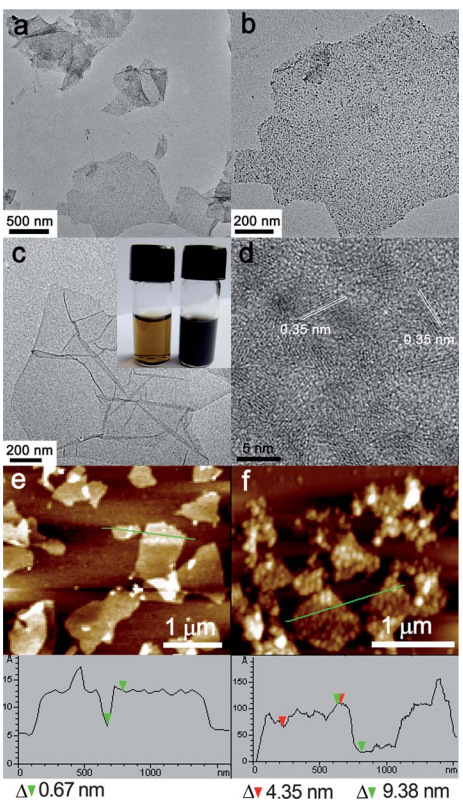

Fig. 1 (a) TEM image of ATG. (b) Magnified TEM image of a typical ATG. (c) TEM image of GO, photograph of the GO (left) and ATG (right) in inset. (d) HRTEM image of ATG, lattice spacing discussed in text is indicated. (e) AFM images of the GO and (f) ATG.

State Key Laboratory of Analytical Chemistry for Life Science, School of Chemistry and Chemical Engineering, Nanjing University, Nanjing, 210093, P. R. China. E-mail: jianglp@nju.edu.cn; Fax: +86-25-8359-7204; Tel: +86-25-8359-7204

† This article is part of a web theme in *Analyst* and *Analytical Methods* on Future Electroanalytical Developments, highlighting important developments and novel applications. Also in this theme is work presented at the Eirelec 2011 meeting, dedicated to Professor Malcolm Smyth on the occasion of his 60th birthday.

‡ Electronic supplementary information (ESI) available: Experimental Details, Zeta potential of ATG, EDS spectra, Nyquist plots and UV-vis spectra of Hb. See DOI: 10.1039/c2ay05781f

TiO_2 nanoparticles on the GR nanosheets. In the acid reaction condition, TiO_2 nanoparticles were protonated and positively charged by the adsorbed HNO_3 (zeta potential 21.3 mV, Fig. S1‡), and the dispersibility of ATG was enhanced due to the electrostatic force.[11] As shown in the highly magnified TEM image (Fig. 1b), the GR sheet is densely covered with ~5 nm TiO_2 nanoparticles. In comparison with GO (Fig. 1c), the surface of ATG is much rougher than that of GO, which can be attributed to the existence of TiO_2 nanoparticles on the GR sheet. The photograph of GO (left) and ATG (right) solutions is shown in the inset of Fig. 1c. The colour of the solution shifts from brown to black, which indicates the reduction of GO to GR. High resolution-TEM image (Fig. 1d) further confirms the crystalline TiO_2 nanoparticles spreading over the GR surface. The fringes with a lattice spacing of 0.35 nm can be indexed as the (101) plane of anatase TiO_2. Energy-dispersive spectroscopy analysis for different regions also confirmed the existence of TiO_2 species on the graphene (Fig. S2‡). Fig. 1e and Fig. 1f depict the typical atomic force microscope (AFM) images of GO and ATG. The thickness of GO, measured from the height profile of the AFM image is about 0.67 nm (Fig. 1e), which is consistent with the data of single layered GO.[1,9] ATG exhibits a rougher surface than GO, which arises from the binding of 4.35 nm TiO_2 to the GO surface (Fig. 1f). The thickness of graphene in ATG nanocomposites can be calculated from the thickness of ATG (9.38 nm) and diameter of TiO_2 (4.35 nm), and a value of 0.68 nm is obtained.

The X-ray powder diffraction (XRD) pattern (Fig. 2a) shows that GO (curve A) has a peak centered at 10.5°. After the reaction with $TiCl_3$, the characteristic peak of GO at 10.5° disappears, indicating the complete reduction of GO. The XRD pattern of ATG (curve B) also confirms the formation of anatase TiO_2 (JCPDS, No. 84-1286) with an estimated crystalline size of 4.5 nm.[12] Furthermore, Fourier-transform infrared spectroscopy was employed to investigate the formation of ATG. As shown in Fig. 2b, ATG (curve C) shows an obvious skeletal vibration adsorption band of the GR sheets at 1623 cm^{-1}, similar to that of GR (1630 cm^{-1}, curve B).[1,6,10] The absence of the peaks at 1730 cm^{-1} (C═O), 1385 cm^{-1} (C–OH) and 1060 cm^{-1} (C–O) indicates the removal of oxo-groups on GO (curve A) after reduction. The broad absorption at 500–800 cm^{-1} corresponds to the characteristic vibrations of Ti–O–Ti bands of TiO_2, the same as P25 (curve D), indicating the existence of TiO_2.[6,10] The Raman spectrum of ATG also confirms the reduction of GO. As shown in Fig. 2c, from GO (curve B) to ATG (curve A), the ratio of D/G increases significantly, indicating the decrease in the average size of the sp^2 domains upon reduction of the exfoliated GO.[4,10,13] It can be concluded that the titanium(III) ion has enough reducing ability to convert GO into GR, and finally the ATG nanocomposites formed.

Since graphene is a good electron acceptor with outstanding electron mobility, the introduction of graphene might enhance the transfer of electrons. To investigate the charge carriers transfer behavior of ATG, electrochemical impedance spectra measurements were carried out. The electron transfer resistance decreased from 48.2 Ω for the P25 to 18.3 Ω for ATG and 16.8 Ω for GR, respectively (Fig. S3‡). It indicates that with the introduction of graphene, the interface resistance and charge transfer resistance on the surface of ATG decrease obviously.[5,6]

Hb, as a model protein, was immobilized on the ATG nanocomposites to explore the applicable approach for the fabrication of biosensors. The electrochemical behavior of the Hb–ATG/GCE was studied by cyclic voltammetry (CV). As is shown in Fig. 3a, no current peak was observed at ATG/GCE (curve D), indicating the electro-inactiveness of ATG nanocomposites in the absence of Hb. Only a small irreversible reduction peak was observed on Hb–GR/GCE and Hb/GCE (Fig. 3a, curve B, C), suggesting the possible denaturation and desorption of Hb on GR/GCE and bare GCE surface. However, Hb–ATG/GCE shows a pair of well-defined and quasi-reversible redox peaks at −0.297 and −0.402 V (*vs.* SCE), respectively (curve A), which are in accordance with the characteristic of Fe^{III}/Fe^{II} redox couples of heme proteins.[14,15] These results demonstrate that the DET between Hb and GCE could be improved by the introduction of ATG nanocomposites. For these ATG nanocomposites, GR established high specific surface areas and a fast electron transfer path to facilitate the DET of Hb, and TiO_2 nanoparticles provided more absorption sites and good biocompatible microenvironment for the loading of Hb and the retaining of native bioactivity.

The effect of scan rate has also been investigated (Fig. 3b), and both the oxidation and reduction peak currents increased linearly with the scan rates from 20 to 1000 mV s^{-1}, indicating a surface-controlled electrode process. According to Faraday's law, the average surface coverage (Γ*) of Hb on the surface of ATG was estimated to be 2.15×10^{-9} mol cm^{-2}, which was much larger than that of theoretical monolayer coverage of Hb ($\sim 1.89 \times 10^{-11}$ mol cm^{-2}).[15] The loading amount of Hb can be calculated from the UV-Vis spectra of the Hb solution before and after the assembly with ATG (Fig. S4‡). The loading amount Hb in the Hb–ATG can be calculated to $1.29 \bullet 10^{-2}$ mg. These results demonstrated that ATG had a high adsorption capacity, and therefore, favoured the immobilization of Hb.

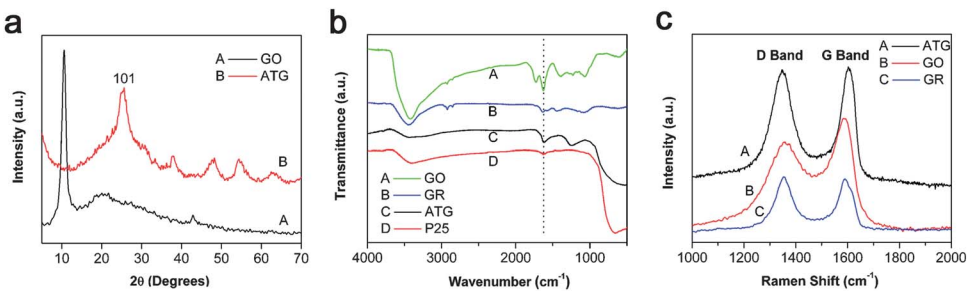

Fig. 2 (a) The XRD patterns of (A) GO and (B) ATG. (b) The FT-IR spectra of (A) GO, (B) GR, (C) ATG and (D) P25. (c) The Raman spectra of (A) ATG, (B) GO and (C) GR.

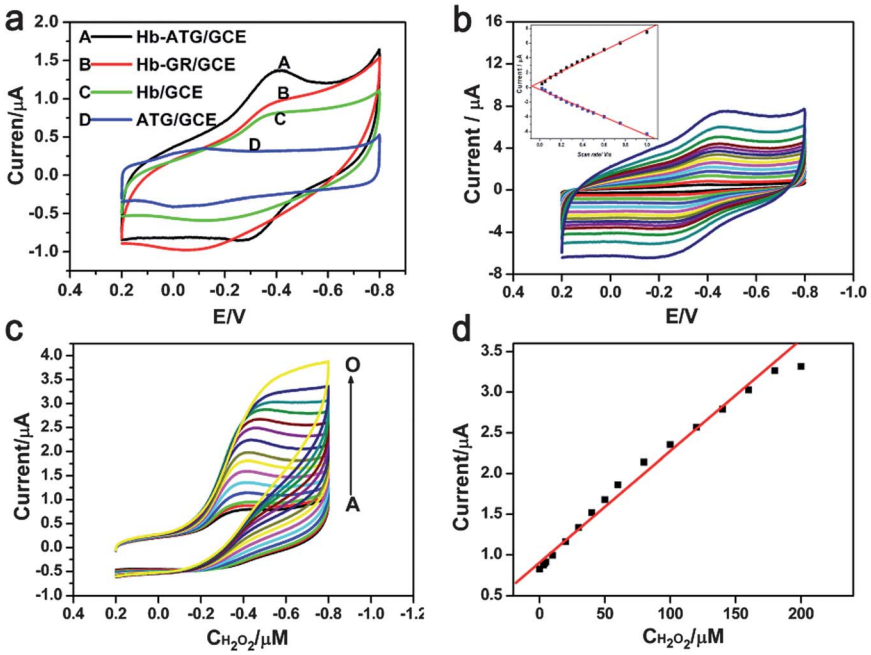

Fig. 3 (a) CVs of Hb–ATG/GCE (A), Hb–GR/GCE (B), Hb/GCE (C) and ATG/GCE (D) in 0.1 M pH 7.0 PBS solution. (b) CVs of Hb–ATG/GCE in PBS (0.1 M, pH 7.0) at different scan rates (from inner to outer curve: 20, 50, 100, 150, 200, 250, 300, 350, 400, 450, 500, 600, 750, 1000 mV s^{-1}), and plots of cathodic and anodic peak currents *vs.* scan rates (inset). (c) CVs of the Hb–ATG/GCE at scan rate of 0.1 V s^{-1} in 0.1 M pH 7.0 PBS solution with, from bottom to top curve, A-O: 0, 5, 10, 20, 30, 40, 50, 60, 80, 100, 120, 140, 160, 180, 200 μM H_2O_2. (d) Linear plot of electrocatalytic current *vs.* H_2O_2 concentration.

The Hb–ATG/GCE exhibits good electrocatalytic activity toward the reduction of H_2O_2. As is shown in Fig. 3c, with gradual additions of H_2O_2, the reduction peak increased gradually. These characteristics are the typical features of electrocatalytic reactions. The reductive i_p has a good linear relationship with the concentration of H_2O_2 from 3 to 180 μM and attains saturation levels at higher concentrations (Fig. 3d), representing a typical Michaelis–Menten enzymatic reaction characteristic. The detection limit is estimated to be *ca.*1.5 μM (S/N = 3). The apparent Michaelis–Menten constant (K_M^{app}) is estimated to be 63.67 μM from the Lineweaver–Burke equation,[14] which is much smaller than those previously reported,[15,17–20] indicating that the immobilized Hb possesses higher enzymatic activity and the Hb–ATG/GCE exhibits a higher affinity for H_2O_2. Therefore, the ATG nanocomposites provide favourable microenvironment for Hb to perform the DET and good catalytic activity to H_2O_2. It should also be pointed out that Hb–ATG/GCE displays good reproducibility and stability with a relative standard deviation of 2.7% for seven independent determinations for 50 μM H_2O_2 solution, and the biosensor retained *ca.* 92% of initial response to 20 μM H_2O_2 after a month.

In summary, ATG with good conductivity, solubility and biocompatibility were successfully synthesized by a one-step facile method. By combining the advantages of TiO_2 and GR, the proposed biosensor showed an enhanced DET of Hb. Moreover, it also displayed excellent analytical performance in the determination of H_2O_2 with wide linear range and low detection limit. The as-synthesized ATG can be a potential material used for the immobilization of biomolecules, and development of third-generation biosensors with good reproducibility and stability.

We are grateful to the financial support of the National Natural Science Foundation of China (Nos. 21073084, 21075061, 21105050), "973" Program (Nos. 2011CB933502, 2007CB936302), the Foundation of the Jiangsu Education Committee (11KJB150011) and the Natural Science Foundation of Jiangsu Province (BK2010363). We also appreciate the support of the Fundamental Research Funds for the Central Universities (1105020503, 1116020507 and 1112020504) and the State Key Laboratory of Analytical Chemistry for Life Science (SKLACLS1105).

Notes and references

1 K. S. Novoselov, A. K. Geim, S. V. Morozov, D. Jiang, Y. Zhang, S. V. Dubonos, I. V. Grigorieva and A. A. Firsov, *Science*, 2004, **306**, 666.
2 A. K. Geim and K. S. Novoselov, *Nat. Mater.*, 2007, **6**, 183.
3 X. L. Li, G. Y. Zhang, X. D. Bai, X. M. Sun, X. R. Wang, E. Wang and H. J. Dai, *Nat. Nanotechnol.*, 2008, **3**, 538.
4 H. L. Guo, X. F. Wang, Q. Y. Qian, F. B. Wang and X. H. Xia, *ACS Nano*, 2009, **3**, 2653.
5 D. H. Wang, D. W. Choi, J. Li, Z. G. Yang, Z. M. Nie, R. Kou, D. H. Hu, C. M. Wang, L. V. Saraf, J. G. Zhang, I. A. Aksay and J. Liu, *ACS Nano*, 2009, **3**, 907.
6 H. Zhang, X. J. Lv, Y. M. Li, Y. Wang and J. H. Li, *ACS Nano*, 2010, **4**, 380.
7 G. Williams, B. Seger and P. V. Kamat, *ACS Nano*, 2008, **2**, 1487.
8 C. Chen, W. M. Cai, M. C. Long, B. X. Zhou, Y. H. Wu, D. Y. Wu and Y. J. Feng, *ACS Nano*, 2010, **4**, 6425.
9 C. Z. Zhu, S. J. Guo, P. Wang, L. Xing, Y. X. Fang, Y. M. Zha and S. J. Dong, *Chem. Commun.*, 2010, **46**, 7148.
10 K. F. Zhou, Y. H. Zhu, X. L. Yang, X. Jiang and C. Z. Li, *New J. Chem.*, 2011, **35**, 353.
11 Z. Wang, T. Yamaguchi, H. Sugihara and H. Arakawa, *Langmuir*, 2005, **21**, 4272.
12 B. D. Cullity, *Elements of X-ray diffraction*, 2nd ed., Addison-wesley, Reading, MA, 1978, p.102.

13 S. Stankovich, D. A. Dikin, R. D. Piner, K. A. Kohlhaas, A. Kleinhammes, Y. Y. Jia, Y. Wu, S. T. Nguyen and R. S. Ruoff, *Carbon*, 2007, **45**, 1558.
14 H. Zhang, J. J. Xu and H. Y. Chen, *J. Phys. Chem. C*, 2007, **111**, 16564.
15 H. Zhang, J. J. Xu and H. Y. Chen, *J. Electroanal. Chem.*, 2008, **624**, 79.
16 R. A. Kamin and G. S. Wilson, *Anal. Chem.*, 1980, **52**, 1198.
17 J. J. Zhang, Y. G. Liu, L. P. Jiang and J. J. Zhu, *Electrochem. Commun.*, 2008, **10**, 355.
18 Y. Y. Wang, X. J. Chen and J. J. Zhu, *Electrochem. Commun.*, 2009, **11**, 326.
19 H. Y. Zhao, W. Zheng, Z. X. Meng, H. M. Zhou, X. X. Xua, Z. Li and Y. F. Zheng, *Biosens. Bioelectron.*, 2009, **24**, 2356.
20 H. F. Xu, H. Dai and G. N. Chen, *Talanta*, 2010, **81**, 337.

